



**HAL**  
open science

# Directed self-assembly in “breath figure” templating of block copolymers followed by soft hydrolysis-condensation: One step towards synthetic bio-inspired silica diatoms exoskeleton

Antoine Aynard, Laurence Pessoni, Laurent Billon

## ► To cite this version:

Antoine Aynard, Laurence Pessoni, Laurent Billon. Directed self-assembly in “breath figure” templating of block copolymers followed by soft hydrolysis-condensation: One step towards synthetic bio-inspired silica diatoms exoskeleton. *Polymer*, 2020, 210, pp.123047. 10.1016/j.polymer.2020.123047. hal-02950386

HAL Id: hal-02950386

<https://univ-pau.hal.science/hal-02950386v1>

Submitted on 23 Sep 2022

**HAL** is a multi-disciplinary open access archive for the deposit and dissemination of scientific research documents, whether they are published or not. The documents may come from teaching and research institutions in France or abroad, or from public or private research centers.

L'archive ouverte pluridisciplinaire **HAL**, est destinée au dépôt et à la diffusion de documents scientifiques de niveau recherche, publiés ou non, émanant des établissements d'enseignement et de recherche français ou étrangers, des laboratoires publics ou privés.



Distributed under a Creative Commons Attribution - NonCommercial 4.0 International License

## Directed self-assembly in "breath figure" templating of block copolymers followed by soft hydrolysis-condensation: one step towards synthetic bio-inspired silica diatoms exoskeleton

Antoine Aynard,<sup>a,b</sup> Laurence Pessoni,<sup>a,b</sup> Laurent Billon<sup>a,b\*</sup>

<sup>a</sup>Université de Pau et Pays de l'Adour, E2S UPPA, CNRS, Institut des Sciences Analytiques & de PhysicoChimie pour l'Environnement & les Matériaux, UMR5254, 64000, PAU, France

<sup>b</sup>Bio-inspired Materials group: Functionalities & Self-assembly, E2S UPPA, Hélioparc, 2 avenue Angot, 64053, PAU, France.

\*Corresponding Author.

*E-mail address:* laurent.billon@univ-pau.fr

*Keywords:* Self-assembly, breath figure, bottom-up process, sol-gel, bio-inspired materiel

### Abstract

Structural and chemical bio-inspired silica honeycomb films were obtained by combination of the directed self-assembly in "breath figure" templating to create honeycomb film and the post hydrolysis-condensation of a block copolymer PolyStyrene-*block*-Poly(3-(Trialkyloxysilyl)propyl methacrylate)) PS-*b*-PTEPM. Then pyrolysis at moderate temperature was used to achieve the elaboration of hierarchically porous silica film as bio-inspired diatoms frustules. In this work, block copolymers PS-*b*-PTEPM were synthesized by Nitroxide Mediated Polymerization to create honeycomb film by a "breath figure" bottom-up process. The PS block allows the formation of microporous film whereas the PTEPM block leads to the silica nanophase by *in situ* soft sol-gel reaction. The copolymer PS<sub>0.34</sub>-*b*-PTEPM<sub>0.66</sub> allows the formation of a nicely patterned honeycomb film with nanocylinders of PS in a matrix of PTEPM. After soft hydrolysis-condensation and pyrolysis processes, a hierarchically-structured and fully inorganic honeycomb film is created as a synthetic bio-inspired silica diatom frustules.

## 1. Introduction

Porous material presents several points of interest, thanks to their high specific surface, in the field of sensors,[1] bio-sensors,[2] catalysis,[3] photocatalysis,[4] separation and purification techniques[5,6] or even in electronics.[7] Porous materials can be obtained by many top-down or bottom-up approaches. However, most are time consuming and require several steps. The breath figure (BF) process, discovered by François and coworkers,[8–10] was used by other groups to generate pore at a micron scale in one step.[11–17] Billon and coworkers demonstrated that new levels of structuration can be obtained inside the pore leading then to hierarchically structured honeycomb films.[18–20] The structuration at the nanoscale inside the walls, in between the micropores, is attributed to the ability of a block copolymer to self-assemble into several nanostructures such as lamellae, cylinders, gyroids or spheres.[21,22] The directed self-assembly in “breath figure” templating of the diblock copolymers emphasizes the compatibility of kinetics between these two processes since no annealing was required. It is worth noting that the micro-porous films with internal nano-structuration can be generated using large range of diblock copolymers designs.[19,20,23–27] Also, one of the two blocks can be a sacrificial component[28] leading to two levels of porosities by *in situ* degradation.[29,30]

In Nature, an alga called diatom is particularly fascinating scientists and is the source of numerous studies. Indeed, this microscopic alga is composed of a highly porous and rigid cell walls, i.e. frustules, made of amorphous silica.[31] The silica structures formed by diatoms is one of the most stunning examples of biological nanofabrication and source of inspiration on conditions close to ambient, i.e. soft chemistry, to mimic chemistry of Nature.[32,33] To our knowledge, there is no report referring to the *in situ* formation of silica honeycomb film by soft conditions, without honeycomb film covering as a template. Indeed, honeycomb films of poly(styrene)-*b*-poly(4-vinylpyridine) was used by Wu *et al.*[26] as template and then

recovered with SiO<sub>2</sub>. A similar approach was used by Zheng *et al.*[34] with a crosslinked poly(acrylic glycidyl ether) honeycomb film as template for an SiO<sub>2</sub> honeycomb film. A “gelable” monomer in block copolymers self-assembly, i.e. 3-(Trialkyloxysilyl)propyl methacrylate (TEPM) or 3-acryloxypropyltriethoxysilane (APTES) monomers, as crosslinking agents have been already used to *in-situ* generate a bulk silica network at room-temperature by sol-gel process.[35–40] The final structuration could be frozen through an acidic sol-gel reaction without damaging the initial morphologies.[39,40]

Herein, the goal is to mimic both the structuration and the chemical composition of the diatom’s exoskeleton by *in-situ* formation of a silica honeycomb film. Thus, poly(styrene)-*block*-poly 3-(triethoxysilyl) propyl methacrylate PS-*b*-PTEPM diblock copolymers were synthesized (ESI†). The PS block was used for his ability to generate highly patterned honeycomb film at the micron scale in the breath figure templating [41,42] while the PTEPM block was hydrolyzed and then crosslinked into silica material by soft sol-gel chemistry. Finally, the PS phase could be removed by a thermal treatment to obtain a fully inorganic bio-inspired porous film.

## 2. Results and discussion

Synthetic bio-inspired silica diatoms exoskeleton means to be able to mimic in an all-in-one material, both its chemistry and also structures. To achieve this goal, a PS<sub>0,55</sub>-*b*-PTEPM<sub>0,45</sub> block copolymer was used as a building block for the elaboration of an inorganic honeycomb film. This block copolymer was synthesized by chain extension under Nitroxide Mediated Polymerization using a PS block (M<sub>n</sub> = 24 000 g.mol<sup>-1</sup>, *D* = 1.23) as macro-initiator with TEPM functional monomers (**Figure SI-1 to SI-6, ESI**). The molecular weight M<sub>n</sub> increases to 51 200 g.mol<sup>-1</sup> with a broad dispersity of *D* = 5.8 (**Figure 1B**). During the polymerization process, the radical concentration keeps constant versus time, thus, dispersity should be

smaller. Therefore, the broad dispersity can be attributed to a preliminary hydrolysis/condensation of the PS-*b*-PTEPM diblock copolymer and then a resulting cross-linking reaction between macromolecular chains or macromolecular chains adsorption on the column. The molecular weight of the final PS-*b*-PTEPM was determined around 80 000 g.mol<sup>-1</sup> by <sup>1</sup>H NMR (**Figure SI-6, ESI**) and an unique diffusion coefficient, without any side products as PS macro-initiator as (**Figure 1A**) confirming the block copolymer architecture. The final molar ratio determined is then 55 % of PS and 45 % of PTEPM. The calculated weight fraction is 34 and 66 % of PS and PTEPM, respectively, corresponding theoretically to cylinders of PS in a PTEPM matrix and confirmed by AFM image a mix of *in-the-plane* and *out-of-the-plane* cylinders (**Figure 1C**).

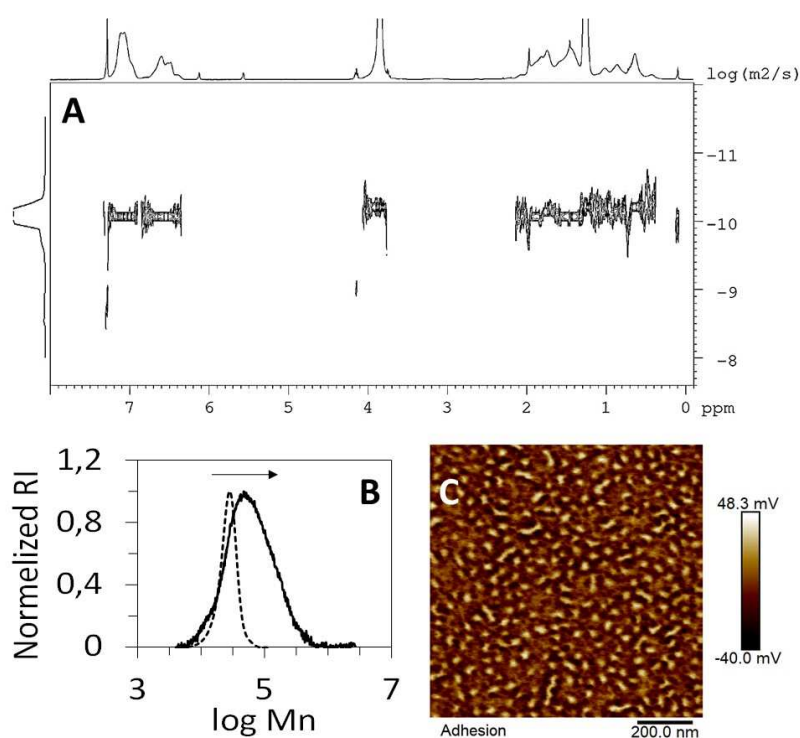


**Figure 1.** <sup>1</sup>H NMR DOSY (A) and SEC traces of PS macroinitiator (dotted line) and PS-*b*-PTEPM (black line) (B). AFM image of the block copolymer self-assembly in thin film (spin coating at 1 000 revolution.min<sup>-1</sup> during 1 min and without any annealing) (C).

Thus, this block copolymer PS-*b*-PTEPM allows the formation of well-ordered honeycomb structure by the breath figure process with pores from 4 to 4.5 μm diameters and a 4 μm

distance between the centers of the pores (**Figure 2A**). A second structuration level at the nano scale is observed by AFM on the surface of the honeycomb film, with a mixture of *out-of-the-plane* and *in-the-plane* PS cylinders (25-30 nm) inside the wall in between micron-sized pores (**Figure 2B**). The thickness of the film is around 5  $\mu\text{m}$  for three layers of pores. Thanks to its thin thickness, the nano-structuration can be also observed on the bottom of pores (**Figure SI-7, ESI**).

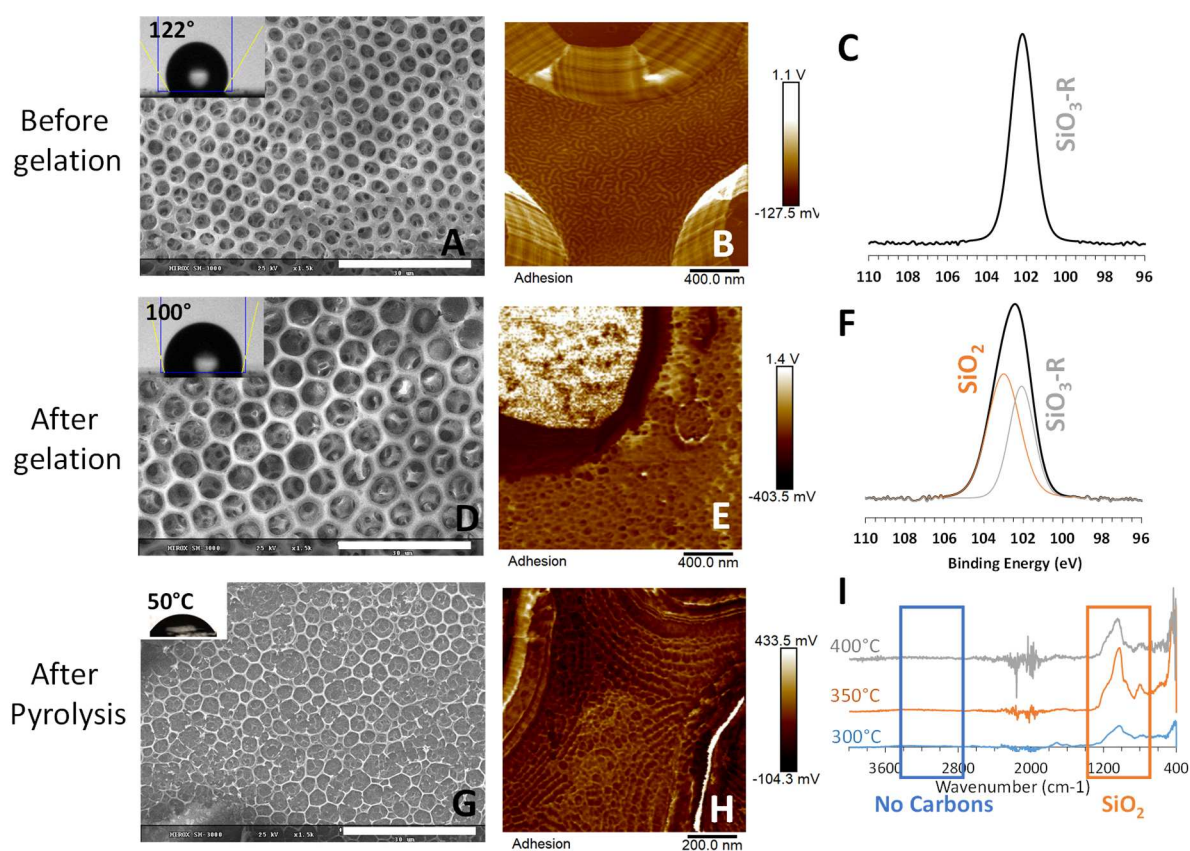


**Figure 2.** SEM images of PS-*b*-PTEPM honeycomb film before (A), after (D) gelation and after pyrolysis (G) (scale bar = 30  $\mu\text{m}$ ) (insert: water droplet **apparent contact angle**); AFM images of PS-*b*-PTEPM honeycomb film before (B), after (E) gelation and after pyrolysis (H) in adhesion; XPS spectra of the Si2p peaks: before (C) and after (F) gelation; FTIR spectrum (I) of the PS-*b*-PTEPM after pyrolysis at 300°C (blue), 350°C (orange) and 400°C (grey).

In order to crosslink the alkoxyisilyl functions and *in-situ* create a bulk inorganic/organic material, the hierarchically structured honeycomb films were hydrolysed and then condensed. The sol-gel crosslinking process was performed in an acidic medium to catalyse the formation

of silica. The gelation effectiveness was followed by TGA. Indeed, the temperature of degradation  $T_d$  and the residual weight loss  $WLR$  increase after the hydrolysis-condensation process, respectively from 380 to 425 °C and 6.5 to 25.1 % of residue at 700°C (**Figure SI-8, ESI**) and confirm the impact of the alkoxyethyl functions crosslinking. It is worth noting that the theoretical residue value was calculated around 18 weight%.

The gelation treatment was also followed by FTIR (**Figure SI-9, ESI**). Before the hydrolysis step, peaks at 1100/1074  $\text{cm}^{-1}$  (Si-O-C) and 1164/954  $\text{cm}^{-1}$  (O-Ethoxy group) disappear whereas the peak from 1025  $\text{cm}^{-1}$  through 1150  $\text{cm}^{-1}$  due to the Si-O-Si bond appeared confirming the gelation of the alkoxyethyl group. Nevertheless, a peak appearing at 3400  $\text{cm}^{-1}$  due to the Si-OH bond traducing an incomplete condensation. According to Gamys et al. this incomplete condensation is probably due to a macromolecular steric hindrance problem preventing the silanol groups from coming into a sufficiently close proximity to condense.<sup>[34]</sup>

The hydrolysis was also confirmed by XPS measurements (**Tables SI-1 & SI-2, ESI**) with Si2p analysis. Indeed, after hydrolysis, a peak at 103.0 eV due to a silica O-Si-O appears (**Figure 2C & F**). However, the hydrolysis reaction is not complete because of the residual peak at 102.1 eV characteristic of the alkoxyethylane group Si-O-C. This result, confirmed by C1s and O1s analysis (**Figure SI-10, ESI**), traduce a decrease of an alkoxyethylane group content with the formation of a silica network after hydrolysis.

Interesting behavior is the modification of surface wettability associated to the chemical change. We *in-situ* investigated the surface modification by the **apparent contact angle** measurement method *vs* time. This approach consists of casting either neutral or acidic water droplets on a non-crosslinked PS-*b*-PTEPM continuous film and observing the evolution of the **apparent contact angle** value with time. For the neutral water droplet, the slight decrease of the **apparent contact angle** value with time from 90 to 80°, i.e. 10°, can be associated to low

evaporation phenomenon. For the acidic droplet, the decrease drops  $40^\circ$  after 60 minutes (from  $90$  to  $50^\circ$ ), corresponding to a progressive formation of the silica network (**Figure 3**).

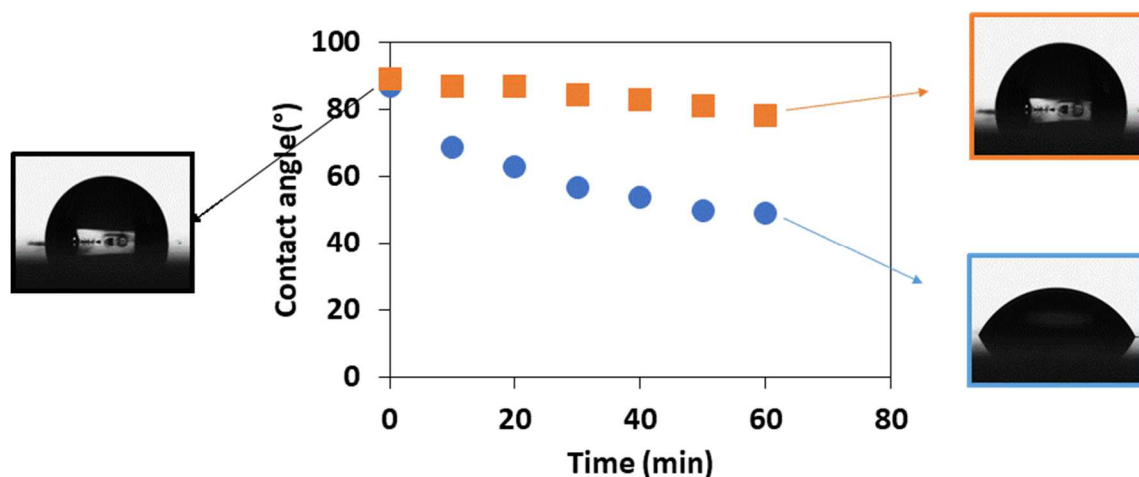


**Figure 3.** *In-situ* hydrolysis by on-line evolution of the **apparent contact angle** of a neutral (orange square) and an acidic droplet (blue circle) onto a non-hydrolyzed continuous film (the experiment was performed in an enclosed box with a constant relative humidity of 95 % at  $20^\circ\text{C}$  for avoiding water evaporation).

**Apparent contact angle** measurements were performed on PS-*b*-PTEPM honeycomb and continuous films. After hydrolysis, a significant decrease of the **apparent contact angle** value is observed from  $122$  to  $100$  and  $86$  to  $56^\circ$  for both honeycomb and continuous films, respectively (**Figure 2 & Table SI-3, ESI**). These phenomena confirm the success of the crosslinking of alkoxy silyl groups and the formation of a hydrophilic silica network.

The hydrolysis/condensation process does not only affect the chemical structure but also the nano and micro-structure. Although the honeycomb structuration is conserved after gelation, the pores diameter slightly changes from  $4.5$  to  $6\ \mu\text{m}$  before hydrolysis/condensation (**Figure 2A & D**). The shrinking of the pore walls can be explained by the loss of the ethoxy groups and the silanol condensation. In the same time, the *out-of-the/in-the-plan* cylinders disappear and make room for spherical nano-domains of  $30\ \text{nm}$  in diameter and a rough surface (**Figure 2E**). This roughness can be caused by the nucleation and growth of silica

particles at the wall surface of the honeycomb films. In Nature, diatoms have similarly nanograins in the body of micrometer-scale framework.

In order to obtain a fully inorganic porous film (**Figure 2G & SI-11, ESI**) a moderate pyrolysis isothermal treatment, nevertheless out of the scope of bio-inspiration, was performed at different temperatures (**Figure SI-12, ESI**). To avoid, strong mechanical constraint and the rupture of the honeycomb, we chose to progressively heat until 400°C. FTIR analysis allows to validate the degradation of the organic matter and the mineralisation. Indeed, characteristic peaks of the original organic materials between 600-950, 1100-1800 and 2800-3200  $\text{cm}^{-1}$  totally disappeared, whereas the silica stretching vibration at 1100  $\text{cm}^{-1}$  remains (**Figure 2I**).

A constant decrease of **apparent contact angle** from 120 to 50° (**Figure 2**) is noticed after pyrolysis, confirming the organic loss towards the highly hydrophilic crosslinked silica network. Nevertheless, this value is higher than pure glass substrate ( $\approx 20^\circ$ ) and is due to the remaining honeycomb structuration observed by SEM (**Figure 2G**). A nano-structuration and roughness are always observed (**Figure 2H and SI-11, ESI**) and are similar to the nano-morphology/roughness observed after the soft hydrolysis-condensation (**Figure 2E**). Herein, we assume a nucleation and growth of silica particles onto the top surface of the honeycomb walls. The removal of the organic matter during the heating lets appear only silica particles leading to a hierarchical structured inorganic film with micron-meter pores surrounded by patterned walls with nano silica-grains.

### **3. Experimental part**

#### ***3.1. Materials and Methods***

3-(triethoxysilyl) propyl methacrylate (TEPM, 97 %) was purchased from ABCR, Styrene ( $S \geq 99 \%$ ) was purchased from Sigma Aldrich. The BlocBuilder® alkoxyamine (2-methylaminoxypionic-SG1) used as the initiator was supplied by Arkema. Methanol, Anhydrous Toluene and Dichloromethane were purchased from VWR. All products were used as received.

**Polymer analysis.** The molecular weight and dispersity of (co)polymers were measured using size exclusion chromatography SEC using THF as eluent (flow rate  $1.0 \text{ mL}\cdot\text{min}^{-1}$ ) at  $30^\circ\text{C}$ . SEC is equipped with a Viscotek VE 5200 automatic injector, a precolumn and two columns (Styragels HR 5E and 4E (7.8' 300 mm)) and 4 detectors: UV-visible spectrophotometer (Viscotek VE 3210), a Multi-angle Light Scattering detector (Wyatt Heleos II), a viscosimeter (Wyatt Viscostar II) and a refractive index detector (Viscotek VE 3580). Polystyrene standards were used to determine the dispersity of the polymers.  $^1\text{H}$  and diffusion order spectroscopy (DOSY) NMR experiments were carried out on a Bruker AVANCE 400 MHz spectrometer in  $\text{CDCl}_3$  at  $25^\circ\text{C}$ . Chemical shifts are reported as ppm downfield from TetraMethyl Silane (TMS).

**Surface analysis.** Scanning electron microscopy (SEM) observation were realized with a Hirox SH-3000 microscope with an accelerated voltage of 25 kV. Atomic Force Microscope (AFM) images were recorded using an AFM MultiMode8® from Bruker®, on peak force modes. X-Ray Photoelectron Spectrometry (XPS) measurements were performed on a Thermo K-alpha spectrometer equipped with a 120 mm mean radius Hemispherical Analyzer (HAS) and a microfocussed monochromated radiation (Al  $\text{K}\alpha$ , 1486.6 eV, microspot continuously variable from 30 to 400  $\mu\text{m}$  diameter) operating under UHV conditions (residual pressure of  $1 \times 10^{-9}$  mbar). The X-ray power was operating at 72 W (12 kV, 6 mA) for a typical 400  $\mu\text{m}$  beam diameter. The spectra were recorded in the constant Pass Energy (PE) mode CAE, both for wide high sensitivity survey spectra (PE = 200 eV) and high energy

resolution analyses (PE = 20 eV) for quantitatively resolved chemical analyses. Charge effects were compensated by the use of a charge neutralisation system (low energy electrons) which had the unique ability to provide consistent charge compensation. All the neutraliser parameters remained constant during analysis and allowed one to find a 285.0 eV C1s binding energy for adventitious carbon. Spectra were mathematically fitted with Casa XPS software using a least squares algorithm and a non-linear baseline. The fitting peaks of the experimental curves were defined by a combination of Gaussian (70 %) and Lorentzian (30 %) distributions. Only core level spectra for the elements with highest photoionization cross section were recorded in order to extract more reliable information. Fourier Transformed InfraRed (FTIR) spectrum were recorded with a Thermo Fisher Nicolet iS50 FTIR Spectrometer in Attenuated Total Reflectance mode (ATR). **The apparent contact angle measurement was realized with an optical device which allow to determine the contact angle of a water droplet with the surface. Each measurement was realized three times on three different films with similar treatments. Whatever the condition was, the maximum deviation observed was 5°, and considers as error for each measurement.**

**Thermal analysis.** Thermogravimetric (TGA) measurements were obtained with a PerkinElmer-TGA 4000 instrument, using a heating rate of 20°C.min<sup>-1</sup>.

### ***3.2. Honeycomb film preparation***

The honeycomb structuration was induced by the Breath Figure process which is a suitable technic to generate pore at a micron scale. In our case, the breath figure process was achieved under static condition. A 5 g.L<sup>-1</sup> solution of PS-*b*-PTEPM in Dichloromethane was casted onto a glass plate and left in a closed box with a humid atmosphere (Relative Humidity between 60 to 65 % RH) during 5 minutes. The remaining solvent and water droplet were then allowed to evaporate under normal condition. All films were analysis by FTIR in ATR mode, XPS, TGA and **apparent contact angle**.

### **3.3. Gelation treatment: hydrolysis/condensation**

Films were introduced into a 2 mol.L<sup>-1</sup> aqueous solution of HCl for 24 hours and heated at 60°C for 12 hours under vacuum. After gelation, films were analyzed by FTIR in ATR mode, XPS and **apparent contact angle**. In order to know the thermal behavior of PS-*b*-PTEPM film, TGA analysis was also realized from their grinding into powder after gelation.

### **3.4. Pyrolysis treatment**

In order to remove the residual organic part of honeycomb films, *i.e.* the methacrylic moieties, the crosslinked film were pyrolyzed in an oven with an air atmosphere. Different thermal conditions were tested at 700°C for 1h, 300°C and 350°C for 6.5h, 400°C for 1h and a gradient ramp of temperature at 20°C.min<sup>-1</sup> from 30°C to 400°C (**Figure SI-12, ESI**). The different residue are 20 % for 700°C, 40 % for 300 and 350°C, 22 % for 400°C and 24 % for the ramp.

## **4. Conclusion**

In this work, we achieved the synthesis of a hybrid organic/inorganic PS-*b*-PTEPM diblock copolymer by NMP. From a 34/66 fraction of PS/PTEPM, nice honeycomb film was generated through a Breath figure on static condition with a water atmosphere. AFM images of the pore walls shows the presence of cylindrical nano-patterns oriented perpendicular and parallel to the plan. This hierarchically structured honeycomb film was then frozen by crosslinking the alkoxysilyl moieties of the PTEPM, by a soft sol-gel process. The chemical modification was followed by FTIR, **apparent contact angle** measurements, TGA and XPS, underlining the successful hydrolysis/condensation. The resulting film was then heated at high temperature to remove all the organic matter and elaborate a fully inorganic porous film. The honeycomb structuration can be conserved and the nucleation/growth of silica nodules observed leading to a hierarchically structured silica honeycomb film mimicking the nature of

the matter and the structure of the diatom exoskeleton. Nevertheless, the thermal degradation of the PS phase does not fully mimic the diatom bio-process. Some works are underway to replace the PS block by a polymer more compatible with soft chemistry to create a hierarchically porous silica honeycomb film.

### **Acknowledgements**

The authors thank Dr A. Khoukh for NMR analysis, Ass. Prof. J.C. Dupin for XPS characterization and V. Pellerin for SEM images. Dr P. Marcasuzaa is warmly thanked for his discussion.

### **References**

- [1] C.-B. Park, Y.-H. Lee, S.-B. Yi, Fabrication of porous polymeric film for humidity sensing, *Sensors and Actuators: B. Chemical*. 13 (1993) 86–88. [https://doi.org/10.1016/0925-4005\(93\)85330-D](https://doi.org/10.1016/0925-4005(93)85330-D).
- [2] T. Guo, J. Gao, X. Qin, X. Zhang, H. Xue, A novel glucose biosensor based on hierarchically porous block copolymer film, *Polymers*. 10 (2018). <https://doi.org/10.3390/polym10070723>.
- [3] P. Kaur, J.T. Hupp, S.T. Nguyen, Porous organic polymers in catalysis: Opportunities and challenges, *ACS Catalysis*. 1 (2011) 819–835. <https://doi.org/10.1021/cs200131g>.
- [4] L. Pessoni, S. Lacombe, L. Billon, R. Brown, M. Save, Photoactive, porous honeycomb films prepared from rose bengal-grafted polystyrene, *Langmuir*. 29 (2013). <https://doi.org/10.1021/la402079z>.
- [5] K. Lewandowski, P. Murer, F. Svec, J.M.J. Fréchet, The Design of Chiral Separation Media Using Monodisperse Functionalized Macroporous Beads: Effects of Polymer Matrix, Tether, and Linkage Chemistry, *Analytical Chemistry*. 70 (1998) 1629–1638.

<https://doi.org/10.1021/ac971196x>.

- [6] A.H. Dabwan, D. Imai, S. Kaneco, I. Senmatsu, K. Nakahama, H. Katsumata, T. Susuki, K. Ohta, Water purification with sintered porous materials fabricated at 400°C from sea bottom sediments, *Journal of Environmental Sciences*. 20 (2008) 172–176. [https://doi.org/10.1016/S1001-0742\(08\)60027-3](https://doi.org/10.1016/S1001-0742(08)60027-3).
- [7] L. Heng, J. Zhai, Y. Zhao, J. Xu, X. Sheng, L. Jiang, Enhancement of photocurrent generation by honeycomb structures in organic thin films, *ChemPhysChem*. 7 (2006) 2520–2525. <https://doi.org/10.1002/cphc.200600393>.
- [8] G. Widawski, M. Rawiso, B. François, Self-organized honeycomb morphology of star-polymer polystyrene films, *Nature*. 369 (1994) 387. <http://dx.doi.org/10.1038/369387a0>.
- [9] B. François, O. Pitois, J. François, Polymer films with a self-organized honeycomb morphology, *Advanced Materials*. 7 (1995) 1041–1044. <https://doi.org/10.1002/adma.19950071217>.
- [10] O. Pitois, B. François, Formation of ordered micro-porous membranes, *European Physical Journal B*. 8 (1999) 225–231. <https://doi.org/10.1007/s100510050685>.
- [11] P. Escalé, L. Rubatat, L. Billon, M. Save, Recent advances in honeycomb-structured porous polymer films prepared via breath figures, *European Polymer Journal*. 48 (2012) 1001–1025. <https://doi.org/10.1016/j.eurpolymj.2012.03.001>.
- [12] Y. Dou, M. Jin, G. Zhou, L. Shui, Breath figure method for construction of honeycomb films, *Membranes*. 5 (2015) 399–424. <https://doi.org/10.3390/membranes5030399>.
- [13] A. Muñoz-Bonilla, M. Fernández-García, J. Rodríguez-Hernández, Towards hierarchically ordered functional porous polymeric surfaces prepared by the breath figures approach, *Progress in Polymer Science*. 39 (2014) 510–554. <https://doi.org/10.1016/j.progpolymsci.2013.08.006>.

- [14] L. Heng, B. Wang, M. Li, Y. Zhang, L. Jiang, Advances in fabrication materials of honeycomb structure films by the breath-figure method, *Materials*. 6 (2013) 460–482. <https://doi.org/10.3390/ma6020460>.
- [15] E. Bormashenko, R. Pogreb, O. Stanevsky, Y. Bormashenko, T. Stein, O. Gengelman, Mesoscopic patterning in evaporated polymer solutions: New experimental data and physical mechanisms, *Langmuir*. 21 (2005) 9604–9609. <https://doi.org/10.1021/la0518492>.
- [16] N. Maruyama, T. Koito, J. Nishida, T. Sawadaishi, X. Cieren, K. Ijro, O. Karthaus, M. Shimomura, Mesoscopic patterns of molecular aggregates on solid substrates, *Thin Solid Films*. 327–329 (1998) 854–856. [https://doi.org/10.1016/S0040-6090\(98\)00777-9](https://doi.org/10.1016/S0040-6090(98)00777-9).
- [17] O. Karthaus, N. Maruyama, X. Cieren, M. Shimomura, H. Hasegawa, T. Hashimoto, Water-assisted formation of micrometer-size honeycomb patterns of polymers, *Langmuir*. 16 (2000) 6071–6076. <https://doi.org/10.1021/la0001732>.
- [18] P. Escalé, M. Save, A. Lapp, L. Rubatat, L. Billon, Hierarchical structures based on self-assembled diblock copolymers within honeycomb micro-structured porous films, *Soft Matter*. 6 (2010) 3202–3210. <https://doi.org/10.1039/c0sm00029a>.
- [19] P. Marcasuzaa, S. Pearson, K. Bosson, L. Pessoni, J.-C. Dupin, L. Billon, Reactive nano-patterns in triple structured bio-inspired honeycomb films as a clickable platform, *Chemical Communications (Cambridge, England)*. 54 (2018) 13068–13071. <https://doi.org/10.1039/c8cc05333b>.
- [20] P. Marcasuzaa, H. Yin, Y. Feng, L. Billon, CO<sub>2</sub>-Driven reversible wettability in a reactive hierarchically patterned bio-inspired honeycomb film, *Polymer Chemistry*. 10 (2019) 3751–3757. <https://doi.org/10.1039/c9py00488b>.
- [21] F.S. Bates, G.H. Fredrickson, Block copolymer thermodynamics: Theory and

- experiment, *Annual Review of Physical Chemistry*. 41 (1990) 525–557.  
<https://doi.org/10.1146/annurev.pc.41.100190.002521>.
- [22] F.S. Bates, G.H. Fredrickson, Block copolymers-designer soft materials, *Physics Today*. 52 (1999) 32–38. <https://doi.org/10.1063/1.882522>.
- [23] E. Ji, V. Pellerin, F. Ehrenfeld, A. Laffore, A. Bousquet, L. Billon, Hierarchical honeycomb-structured films by directed self-assembly in “breath figure” templating of ionizable “clicked” PH3T-: B -PMMA diblock copolymers: An ionic group/counter-ion effect on porous polymer film morphology, *Chemical Communications*. 53 (2017) 1876–1879. <https://doi.org/10.1039/c6cc09898c>.
- [24] P. Escalé, L. Rubatat, C. Derail, M. Save, L. Billon, PH sensitive hierarchically self-organized bioinspired films, *Macromolecular Rapid Communications*. 32 (2011) 1072–1076. <https://doi.org/10.1002/marc.201100296>.
- [25] P. Escalé, M. Save, L. Billon, J. Ruokolainen, L. Rubatat, When block copolymer self-assembly in hierarchically ordered honeycomb films depicts the breath figure process, *Soft Matter*. 12 (2016) 790–797. <https://doi.org/10.1039/c5sm01774b>.
- [26] B. Wu, M. Zhou, W. Zhang, Y. Liang, F. Li, G. Li, Combined use of breath figures process and microphase separation of PS-: B -P4VP to produce stable porous nanomaterials, *RSC Advances*. 7 (2017) 24914–24924. <https://doi.org/10.1039/c7ra03643d>.
- [27] S. Chen, M.-H. Alves, M. Save, L. Billon, Synthesis of amphiphilic diblock copolymers derived from renewable dextran by nitroxide mediated polymerization: towards hierarchically structured honeycomb porous films, *Polymer Chemistry*. 5 (2014) 5310–5319. <https://doi.org/10.1039/c4py00390j>.
- [28] A.S. Zalusky, R. Olayo-Valles, J.H. Wolf, M.A. Hillmyer, Ordered nanoporous polymers from polystyrene-poly lactide block copolymers, *Journal of the American*

- Chemical Society. 124 (2002) 12761–12773. <https://doi.org/10.1021/ja0278584>.
- [29] R. Takekoh, T.P. Russell, Multi-length scale porous polymers, *Advanced Functional Materials*. 24 (2014) 1483–1489. <https://doi.org/10.1002/adfm.201301693>.
- [30] A. Bertrand, A. Bousquet, C. Lartigau-Dagron, L. Billon, Hierarchically porous bio-inspired films prepared by combining “breath figure” templating and selectively degradable block copolymer directed self-assembly, *Chemical Communications*. 52 (2016) 9562–9565. <https://doi.org/10.1039/c6cc04760b>.
- [31] J. Bradbury, Nature’s Nanotechnologists: Unveiling the Secrets of Diatoms, *PLOS Biology*. 2 (2004) e306. <https://doi.org/10.1371/journal.pbio.0020306>.
- [32] D. Losic, J.G. Mitchell, N.H. Voelcker, Diatomaceous lessons in nanotechnology and advanced materials, *Advanced Materials*. 21 (2009) 2947–2958. <https://doi.org/10.1002/adma.200803778>.
- [33] N. Nassif, J. Livage, From diatoms to silica-based biohybrids, *Chemical Society Reviews*. 40 (2011) 849–859. <https://doi.org/10.1039/c0cs00122h>.
- [34] K. Zheng, D. Hu, Y. Deng, I. Maitloa, J. Nie, X. Zhu, Crosslinking poly(acrylic glycidyl ether) honeycomb film by cationic photopolymerization and its converting to inorganic SiO<sub>2</sub> film, *Applied Surface Science*. 428 (2018) 485–491. <https://doi.org/10.1016/j.apsusc.2017.09.110>.
- [35] P.F.W. Simon, R. Ulrich, H.W. Spiess, U. Wiesner, Block copolymer-ceramic hybrid materials from organically modified ceramic precursors, *Chemistry of Materials*. 13 (2001) 3464–3486. <https://doi.org/10.1021/cm0110674>.
- [36] J. Du, Y. Chen, Hairy nanospheres by gelation of reactive block copolymer micelles, *Macromolecular Rapid Communications*. 26 (2005) 491–494. <https://doi.org/10.1002/marc.200400579>.
- [37] K. Zhang, X. Yu, L. Gao, Y. Chen, Z. Yang, Mesostructured spheres of

- organic/inorganic hybrid from gelable block copolymers and arched nano-objects thereof, *Langmuir*. 24 (2008) 6542–6548. <https://doi.org/10.1021/la800096w>.
- [38] K. Zhang, L. Gao, Y. Chen, Smart organic/inorganic hybrid nanoobjects with controlled shapes by self-assembly of gelable block copolymers, *Macromolecules*. 41 (2008) 1800–1807. <https://doi.org/10.1021/ma7021698>.
- [39] C.G. Gamys, E. Beyou, E. Bourgeat-Lami, P. Alcouffe, L. David, Nanostructured organic-inorganic hybrid films prepared by the sol-gel method from self-assemblies of PS-*b*-PAPTES-*b*-PS triblock copolymers, *Journal of Polymer Science, Part A: Polymer Chemistry*. 49 (2011) 4193–4203. <https://doi.org/10.1002/pola.24861>.
- [40] C.G. Gamys, E. Beyou, E. Bourgeat-Lami, L. David, P. Alcouffe, Tunable morphologies from bulk self-assemblies of poly(acryloxypropyl triethoxysilane)-*b*-poly(styrene)-*b*-poly(acryloxypropyl triethoxysilane) triblock copolymers, *Macromolecular Chemistry and Physics*. 213 (2012) 10–18. <https://doi.org/10.1002/macp.201100507>.
- [41] L. Billon, M. Manguian, V. Pellerin, M. Joubert, O. Eterradosi, H. Garay, Tailoring highly ordered honeycomb films based on ionomer macromolecules by the bottom-up approach, *Macromolecules*. 42 (2009) 345–356. <https://doi.org/10.1021/ma8020568>.
- [42] L. Ghannam, M. Manguian, J. François, L. Billon, A versatile route to functional biomimetic coatings: Ionomers for honeycomb-like structures, *Soft Matter*. 3 (2007) 1492–1499. <https://doi.org/10.1039/b710282h>.

